BIOMARKERS, VOL. 9, NO. 4–5 (JULY–OCTOBER 2004), 364–385

Taylor & Francis
healthsciences

Development of a multivariate statistical model to predict peroxisome proliferation in the rat, based on urinary ^{1}H-NMR spectral patterns

SUSAN C. CONNOR*, MARK P. HODSON, STEPHANIE RINGEISSEN, BRIAN C. SWEATMAN, PAUL J. MCGILL, CATHERINE J. WATERFIELD and JOHN N. HASELDEN

Safety Assessment, GlaxoSmithKline, Park Road, Ware, Hertfordshire, SG12 0DP, UK

Received 11 December 2003, revised form accepted 21 July 2004

A previous report of this work (Ringeissen *et al.* 2003) described the use of nuclear magnetic resonance (NMR) spectroscopy coupled with multivariate statistical data analysis (MVDA) to identify novel biomarkers of peroxisome proliferation (PP) in Wistar Han rats. Two potential biomarkers of peroxisome proliferation in the rat were described, *N*-methylnicotinamide (NMN) and *N*-methyl-4-pyridone-3-carboxamide (4PY). The inference from these results was that the tryptophan-nicotinamide adenine dinucleotide (NAD^+) pathway was altered in correlation with peroxisome proliferation, a hypothesis subsequently confirmed by TaqMan® analysis of the relevant genes encoding two key enzymes in the pathway, aminocarboxymuconate-semialdehyde decarboxylase (EC 4.1.1.45) and quinolinate phosphoribosyltransferase (EC 2.4.2.19). The objective of the present study was to investigate these data further and identify other metabolites in the NMR spectrum correlating equally with PP. MVDA Partial Least Squares (PLS) models were constructed that provided a better prediction of PP in Wistar Han rats than levels of 4PY and NMN alone. The resulting Wistar Han rat predictive models were then used to predict PP in a test group of Sprague Dawley rats following administration of fenofibrate. The models predicted the presence or absence of PP (above an arbitrary threshold of >2-fold mean control) in all Sprague Dawley rats in the test group.

Keywords: proton nuclear magnetic resonance spectroscopy, multivariate statistical data analysis, peroxisome proliferation, rat, tryptophan-nicotinamide adenine dinucleotide pathway, partial least squares, prediction, threshold, peroxisome proliferator-activated receptor, metabolic profile, metabonomics, metabolomics.

Nomenclature: NMR, Nuclear magnetic resonance; MVDA, Multivariate statistical data analysis; PP, Peroxisome proliferation; NMN, *N*-methylnicotinamide; 4PY, *N*-methyl-4-pyridone-3-carboxamide; NAD^+, Nicotinamide adenine dinucleotide; ACMSD, Aminocarboxymuconate-semialdehyde decarboxylase; QAPRT, Quinolinate phosphoribosyltransferase; PLS, Partial least squares or projection to latent structures; PPAR, Peroxisome proliferator-activated receptors; TEM, Transmission electron microscopy; RLW, Relative liver weight; Pxc, Peroxisome count; HPLC, High performance liquid chromatography; WH, Wistar han; SD, Sprague Dawley; LC, Liquid chromatography; AST, Aspartate aminotransferase; ALT, Alanine aminotransferase; ALP, Alkaline phosphatase; CHL, Cholesterol; Gluc, Glucose; Tprot, Total protein; Alb, Albumin; HDL, High density lipoprotein; LDL, Low density lipoprotein; VLDL, Very low density lipoprotein; TRG, Triglycerides; NOESY, Nuclear overhauser enhancement spectroscopy; RD, Relaxation delay; FID, Free induction decay; TSP, Sodium 3-trimethylsilyl-[2,2,3,3-$^{2}H_4$]-1-propionate; PCA, Principal component analysis; PLS-DA, Partial least squares-discriminant analysis; LC/MS, Liquid chromatography/mass spectrometry; LD, Low dose; HD, High dose; TCA, Tricarboxylic acid cycle; PC, Principal component; UV, Unit variance scaling.

*Corresponding author: Susan C. Connor, Safety Assessment, GlaxoSmithKline, Park Road, Ware, Herts SG12 ODP, UK. Tel: (+44) 01920 882345; Fax: (+44) 01920 882679; e-mail: susan.c.connor@gsk.com

Biomarkers ISSN 1354-750X print/ISSN 1366-5804 online © 2004 Taylor & Francis Ltd
http://www.tandf.co.uk/journals
DOI: 10.1080/13547500400006005

Introduction

Peroxisome proliferation (PP) in rodents is characterized by a marked increase in the size and number of hepatocellular peroxisomes. Peroxisome proliferators are also known to cause liver hypertrophy and hyperplasia in rodents and are associated with the incidence of hepatocellular carcinoma. The fibrate hypolipidaemic drugs, used to treat hyperlipidaemia and hypertriglyceridaemia, have been shown to cause PP and hepatocellular carcinoma in rodents (Bybee *et al.* 1990, Bentley *et al.* 1993). This has led to the classification of a number of lipid-lowering drugs as non-genotoxic carcinogens in rodents. Both the PP and lipid-lowering effects of the fibrates are mediated by the Peroxisome Proliferator-Activated Receptor-α (PPARα) but the mechanism underlying hepatic carcinoma formation is unknown. The majority of literature evidence suggests that humans and non-human primates do not form hepatocellular carcinoma after prolonged treatment with fibrates such as fenofibrate, (Ashby *et al.* 1994, Lake 1995a,b, Tucker and Orton 1995). However, recent data in male Cynomolgus monkeys, using clinically relevant doses of fenofibrate, has shown an increase in peroxisome count of up to 3-fold when treated for 15 days (Qualls *et al.* 2003). There is little, if any, evidence for significant PP in humans but a full assessment of human hepatic response to PPARα agonists is hampered by the lack biomarkers of PP and an incomplete understanding of the mechanism of hepatic effects in rodents.

The presence of peroxisome proliferation in laboratory rodents treated with peroxisome proliferators can be either inferred from an increase in liver weight or directly observed using transmission electron microscopy (TEM) techniques. The former measure is at risk of inaccuracies arising from the possible presence of other causes of liver hypertrophy, whilst the latter is both lengthy and resource intensive. Other methods of PP detection include the measurement of peroxisomal enzymes such as catalase, urate oxidase and acyl-CoA oxidase, either in terms of the enzyme activity or protein concentration (using immunohistochemical methods). The methods described above are invasive and time-consuming, precluding longitudinal studies of onset, progression and recovery of PP in the same animals. There is therefore a need for a quick non-invasive predictive method to determine PP in rodents, which can be extrapolated and may have relevance to other species such as primates and ultimately man.

One approach to *in vivo* toxicity screening and prediction, which addresses these needs, is to use proton nuclear magnetic resonance (^{1}H-NMR) spectroscopy and multivariate statistical data analysis (MVDA) to obtain and explore metabolic profiles of biofluids and tissues. NMR-based metabolic profiling, also known as metabonomics and metabolomics, has received increasing attention over the last decade as it can provide a detailed analysis of the changes observed in metabolic profiles of biofluids (Nicholson *et al.* 1999, Nicholson *et al.* 2002). This allows a rapid evaluation of an animal's metabolic response to a drug treatment or disease. A strong advantage of using NMR as an open system for metabolic profiling is the potential for revealing unexpected changes. The prediction of these changes would not be possible without extensive knowledge of the mechanisms underlying efficacy and toxicity of a particular compound. This advantage is facilitated by the ability of NMR to also detect structural information for all hydrogen-containing compounds

present above the detection limit. Using NMR and MVDA as an open system allows for the identification of novel biomarkers or surrogate biomarkers of disease, which may give mechanistic insight and act as a useful adjunct to hypothesis-driven measurements of biomarkers in the same system. This approach may also be used to conduct a more detailed study into the mechanisms underlying processes such as PP and liver carcinoma in rodents compared to primates and man.

In the present study we have used NMR-based metabolic profiling to build predictive models of PP in rats administered with PPAR agonist compounds. PPARα and δ agonists have lipid-lowering pharmacological properties and are known to be associated with PP (Romach *et al.* 2002). PPARγ agonists have been shown to increase insulin sensitivity and are indicated in type II diabetes mellitus, but there is currently no evidence of an association with PP. The compounds chosen for this study include fenofibrate (primarily PPARα activity), GWA (a PPARα agonist), GWB (a PPARδ agonist with some α activity) and GWC (a PPARγ agonist). GWC was included as a negative control with no associated PP.

A large amount of literature data for NMR-based metabolic profiling studies to date have concentrated on examining the major sources of variation in an NMR dataset (Nicholson *et al.* 1989, Anthony *et al.* 1994, Beckwith-Hall *et al.* 1998, Robertson *et al.* 2000, Slim *et al.* 2002). This variation has been used as an indicator of the distance from control metabolic profile of an animal and therefore the degree of toxicity. Whilst this has shown the potential usefulness of the technique to describe the overall well-being of an animal, many of the potential biomarkers highlighted have been similar for relatively diverse toxicological effects and genetic modifications. In the present study we have used prior knowledge of metabolite variability and the effects of feeding, stress and body weight change to delineate these confounding factors to the NMR models of PP. We have combined urine NMR with pathology data to test the contribution of these "non-specific" effects to initial models of PP. Additional models of PP have been constructed without these non-specific factors for use in conjunction with the "full" model.

The NMR multivariate statistical models have been validated using known biological endpoints of PP. In all cases, this included the increase in relative liver weight (RLW) compared to controls and where available, peroxisome counts (Pxc) obtained by TEM. A previous publication has reported some of the results from this study (Ringeissen *et al.* 2003). In the previous study NMR and HPLC (high performance liquid chromatography) analyses revealed increases in urinary and plasma concentrations of *N*-methylnicotinamide (NMN) (16–59-fold in urine with fenofibrate) and *N*-methyl-4-pyridone-3-carboxamide (4PY) (2–3-fold) which directly correlated with PP. Targeted gene expression analysis (TaqMan®) was carried out to support hypotheses drawn from the presence of the two NMR-detected biomarkers NMN and 4PY. The results confirmed a significant down-regulation (up to 11-fold) of aminocarboxymuconate-semialdehyde decarboxylase (ACMSD, EC 4.1.1.45), adding weight to the NMR-based conclusion that the tryptophan-NAD^+ (nicotinamide adenine dinucleotide) pathway regulation was altered in association with PP.

The objective of the present study was to investigate these data further and identify other metabolites in the NMR spectrum correlating equally with PP.

A number of these metabolites were found to be related structurally to NMN and 4PY. The potential was explored for constructing a MVDA model that incorporated all of these metabolites to provide a better prediction of PP in Wistar Han rats than levels of 4PY and NMN alone. The resulting Wistar Han rat predictive models were then used to predict PP in Sprague Dawley rats following administration of fenofibrate.

Materials and methods

Animals and treatments

Full details of the animal protocol and experiments for the main study can be found in Ringeissen *et al,* 2003. All compounds used were synthesized and purified by GSK laboratories. Outlines of the study design and relevant assays are described below:

- Main Study: Wistar Han Rats (Crl:WI(Glx/BRL/Han)BR)/Male, 65–72 days old on day 0, weight range: 256–312 g were obtained from Charles River UK Ltd., Manston Road, Kent, UK. Each animal was randomly allocated to one of the dose groups outlined in table 1.
- Test Study: Sprague Dawley Rats (Crl:CD(SD)IGS BR)/Male, 56–63 days old on day 0, weight range: 293–351 g were obtained from Charles River UK Ltd, Manston Road, Kent, UK. Each animal was randomly allocated to one of the dose groups outlined in table 1. All compounds were given orally as suspensions in 0.5% (w/w) hydroxypropylmethyl–cellulose and 0.1% (w/w) Polysorbate 80 in Phosphate Buffer (pH 7), in a 2 ml dosing volume.

Following a 10 day acclimatization period in the animal house, five animals/group were housed in individual metabolism cages to allow for the continuous collection of urine throughout the study. Animals were dosed for 7 days beginning on day 0 and necropsied on day 7 when tissues were taken for pathology (including TEM of liver samples). Throughout the acclimatization and study periods animals had access to food (Rat and Mouse 1, SDS, Manea, Cambridgeshire, UK) and water *ad libitum*.

Sample collection

The urine sample collection protocol for each study is shown in table 2. All collections were timed to start after dosing and were collected into 1% (w/v) sodium azide solution (1mL) at room temperature.

Table 1. Summary of dosing groups.

Test material[a]	Study number	Rat strain[b]	Group number	Dose (mg/kg)[c]
Control (vehicle only)	1	WH	1	0
GWA (α-agonist)	1	WH	2	0.3
GWA (α-agonist)	1	WH	3	3
GWB (δ-agonist)	1	WH	4	3
GWB (δ-agonist)	1	WH	5	30
GWC (γ-agonist)	1	WH	6	3
GWC (γ-agonist)	1	WH	7	30
Fenofibrate	1	WH	8	10
Fenofibrate	1	WH	9	100
Control (vehicle only)	2	SD	1	0
Fenofibrate	2	SD	2	200

[a]Compounds were administered orally twice daily at 8.00 am and 4.00 pm hours in the Main study and once daily at 8.00 am hours in the Test study.

[b]WH = Wistar Han rat; SD = Sprague Dawley rat.

[c]The low dose of each compound was chosen from in-house data on structural analogues to provide pharmacological effects and the high dose was set 10-fold higher. The high doses chosen were known to cause peroxisome proliferation for fenofibrate and structural analogues of GWA and GWB (Brown *et al.* 1999). GWA has a similar structure (ureido-thioisobutyric acid analogue) and activity to GW9578 (Brown *et al.* 1999). The lower dose level of GWC was chosen as it caused significant reduction in plasma glucose in ZDF rats whilst not activating other PPAR receptors (in-house studies). The higher dose of GWC was not predicted to activate the PPARα.

Table 2. Sample collection protocol for studies 1 and 2.

	Main Study	Test Study
Acclimatization period in animal house	10 days	10 days
Acclimatization period in metabolism cages	3 days	3 days
Urine collection pre-dose	-3 and -2 days 0–8 h only -1 day 0–8 h, 8–16 h, 16–24 h	-3 and -2 days 0–8 h only -1 day 0–8 h, 8–24 h
Continuous urine collection post-dose	0–8 h, 8–16 h and 16–24 h	0–8 h, 8–24 h
Duration post-dose	7 days	7 days
Faeces[a]	Continuous	None
Relative Liver Weights (RLW)	Recorded on all animals	Recorded on all animals
Peroxisome counts	2 animals per group (randomly selected)	2 animals per group (randomly selected)
Blood collection for clinical pathology[b]	Abdominal aorta	Abdominal aorta
Plasma assays include	AST, ALT, ALP, CHL, gluc, Tprot, alb, HDL, LDL, VLDL, TRG.	AST, ALT, ALP, CHL, gluc, Tprot, alb, HDL, LDL, VLDL, TRG.

[a]Compound metabolites were identified in the faeces and urine by mass spectrometry. NMR was then carried out on isolated liquid chromatography fractions of urine where appropriate (Ringeissen *et al.* 2003). Drug-related NMR resonances were then excluded from statistical analysis.

[b]Routine methodologies (Hitachi 917 random discrete analyser) were used for assessment of plasma clinical chemistry parameters.

Key: AST = aspartate aminotransferase; ALT = alanine aminotransferase; ALP = alkaline phosphatase; CHL = cholesterol; gluc = glucose; Tprot = total protein; alb = albumin; HDL = high-density lipoprotein; LDL = low-density lipoprotein; VLDL = very low density lipoprotein; TRG = triglyceride.

Urine volumes were recorded and the samples retained at -80°C until analysed by ^{1}H-NMR spectroscopy.

Selected target organs for histological processing, including liver, kidney, thyroid and adipose tissue, were retained at necropsy. Relative liver weight was calculated by dividing each liver weight by the total body weight for that animal. Samples were fixed in 10% (w/v) phosphate-buffered formalin and embedded in paraffin wax. Sections (4 μm) were cut and stained with Mayer's haematoxylin and eosin for light microscopy. Livers were taken randomly from two animals in each group for TEM (Ringeissen *et al.* 2003). TEM was carried out using a Philips CM10 transmission electron microscope operating at either 40 KV or 60 KV. Only the hepatocytes within six cells of a central vein or bile duct were examined. This was to ensure that mid-zonal cells were not mistakenly examined. The criteria for assessment were that the cells assessed had a visible nucleus and the entire cell boundary. For each animal the number of peroxisomes in 10 cells from both a periportal and a centrilobular area were counted (*i.e.* a total of 20 cells per animal). The mean numbers of the periportal and centrilobular peroxisomes per cell for each animal and the mean number of peroxisomes per cell for each treatment (% control) were calculated.

NMR analysis of urine

Sample preparation procedures have been previously described in Ringeissen *et al.* 2003. Spectra were acquired using a standard presaturation experiment for water suppression which incorporated the first increment of the NOESY pulse sequence:

$$\mathrm{RD} - 90^{\circ} - t_1 - 90^{\circ} - t_m - \text{collect FID}$$

The NMR acquisition parameters have been summarized in table 3. All spectra were referenced to TSP (sodium 3-trimethylsilyl-[2,2,3,3-$^{2}H_4$]-1-propionate) at $\delta_H = 0$ ppm, phased and baseline corrected using XWINNMR software (Bruker Biospin GmbH, Karlsruhe, Germany).

Statistical analysis of NMR data

Data were reduced to 280 integrated regions of 0.04 ppm corresponding to $\delta_H = 10.0$ to 1.48 ppm using AMIX software (Bruker Biospin GmbH, Karlsruhe, Germany). The regions $\delta_H = 4.9$ to 4.7 and

Table 3. NMR acquisition parameters.

Parameter	Main Study	Test Study
Spectrometer	DRX 600	DRX 700
Probe type	TXIA ATMA	TXIA ATMA
Probe temperature	300K	300K
RD relaxation delay	2s	2s
t_1	3 μs	3 μs
t_m	100 ms	100 ms
Number of scans	64	64
Steady-state scans (not saved)	4	4
Data points for acquisition	64K	64K
Spectral width	12 019.23 Hz	14 005.60 Hz
Acquisition time	2.73s	2.34s
Exponential multiplier prior to FT	0.3 Hz	0.3 Hz

6.02 to 5.5 ppm were excluded from analysis because of the high variability in intensity of the water and urea resonances caused by the NMR experimental protocol. The resonances from the NMR internal standard (TSP) were also excluded from the dataset prior to statistical analysis. Variables corresponding to known metabolites of fenofibrate (in the rat) were deleted from the dataset for the fenofibrate dose groups in both Studies 1 and 2. To allow spectrum to spectrum comparison, each NMR variable was scaled to relative intensity by dividing each variable by the sum of all intensities and multiplying by 1000. The intensity sum was calculated after deletion of water, urea, TSP and drug metabolites from the dataset. Both univariate and multivariate statistical analyses were then applied to the vertically-scaled data. Univariate and multivariate analyses were carried out using Excel (Microsoft Corp) and SIMCA-P (V8.0 and 10.02, Umetrics AB, Sweden), respectively.

Univariate analysis

Main Study: The following univariate statistics were calculated for each spectral bucket for each treatment group:

- the group means;
- the standard deviation of the group means;
- a mean fold change for the treatment group relative to control;
- a Student's t-test (2-tailed, unequal variance assumed) for each treatment group against the control group at the same timepoint;
- Pearson's correlation coefficients for the NMR variables (X) versus RLW (Y) at each time point and dose. The significance of each paired correlation was determined using the p value associated with its t statistic where t follows the distribution t_{n-2} and

$$t = \left| r\sqrt{\frac{n-2}{1-r^2}} \right|,$$

where r is Pearson's correlation coefficient and n is the number of observations.

Multivariate data analysis

The first step in the data analysis used the full dataset (minus water, urea, TSP and fenofibrate metabolites) from the Main study. Subsequent analyses used reduced datasets of the Main study which had selected variables removed. A summary of the analyses carried out on each dataset is highlighted in table 4.

Data were mean-centred and scaled so that the variance was equal either to the initial standard deviation of the variables (pareto scaling) or to unit variance by dividing through by the standard deviation of the variable. Principal components analysis (PCA), partial least squares (PLS) and PLS-discriminant analysis (PLS-DA) were then carried out on the Main study Datasets A, B and C to look for patterns in the data.

Creation of marker tables

The most important positive and negative coefficients responsible for the difference between control and treated animals in the PLS-DA models were highlighted for each time-point from 56 h post-dose onwards and approximately ranked in order of size and contribution to the model. Earlier timepoints were

Table 4. A Summary of the Datasets used to create PCA, PLS-DA and PLS models.

Dataset Name	Description	Timepoints	Use
Main Study Dataset A	Water, urea TSP and fenofibrate metabolites[a] deleted (242 spectral regions remaining).	All	Initial exploration of the data, deletion of outliers and observation of patterns in the data using PCA ($n=5$/group).
		Day 7	PLS models to determine correlations with peroxisome proliferation, using training and test set for validation ($n=5$/group).
Main Study Dataset B	Water, urea TSP and fenofibrate metabolites, tricarboxylic acid cycle intermediates, taurine, hippurate, chlorogenic acid metabolites deleted (208 spectral regions remaining).	Day 7	PLS models to determine correlations with peroxisome proliferation, using training and test set for validation ($n=2$/group)
		56 h post-dose until the end of the study	PLS-DA and univariate statistical analysis to determine compound-specific effects ($n=5$/group)
Main Study Dataset C	42 spectral regions included. These regions were selected from the PLS-DA coefficients that distinguished GWA, GWB and fenofibrate samples from controls but were unaffected by GWC.	Day 7	PLS models to determine correlations with peroxisome proliferation, using training and test set for validation ($n=2$/group).
Test Study Dataset	Same spectral regions as for Dataset C from the Main study	Day 7	Values predicted using PLS model for Main Study Dataset C ($n=5$/group)

[a]Chemical shifts of the fenofibrate metabolites observed in urine (Ringeissen *et al.* 2003) were 7.33, 5.72, 7.22, 6.81, 1.49 (metabolite 1) and 7.73, 7.70, 7.54, 6.94 and 1.61 (metabolite 2).

not analysed further as there was very little difference in the spectra relative to controls prior to 2 days post-dose for GWA, GWB and fenofibrate. This is consistent with the expected time course of peroxisome proliferation which is thought to start 2–3 days post-fenofibrate administration. Spectral regions were considered to have minimal influence on the models if their associated PLS-DA coefficients had either a large associated error or appeared on the flat part of the sigmoidal curve after sorting. For each compound a table of important coefficients for each spectral bucket was obtained against time. Univariate t-test p values and mean fold changes were compared with the coefficient ranks to provide additional evidence of the contribution of each spectral bucket for discriminating between groups. Statistically-directed detailed examination of the spectra was then performed and positive/tentative assignments made based on database and literature information. Figure 1 depicts a summary of the above process.

Construction of a predictive model of peroxisome proliferation

Predictive PLS models of peroxisome proliferation were constructed using terminal time-points for Datasets A, B and C from the Main study NMR data and absolute peroxisome counts ($n=2$/group). In all cases the models were validated by randomizing the X and Y pairs and comparing the actual R^2 and Q^2 with those from the simulated examples. Models were accepted as valid if Q^2 fell below zero and the R^2 value also reduced. The models were also tested for over-fit by dividing the Main study dataset (A, B, or C) into two equally populated groups arbitrarily designated training and test sets. The training set was used to construct the model and the Y variable was then predicted for the test set. The training and test set were then swapped and the process repeated. The predicted and observed values were then compared to determine the quality of the models. Model performance was assessed using the error between the

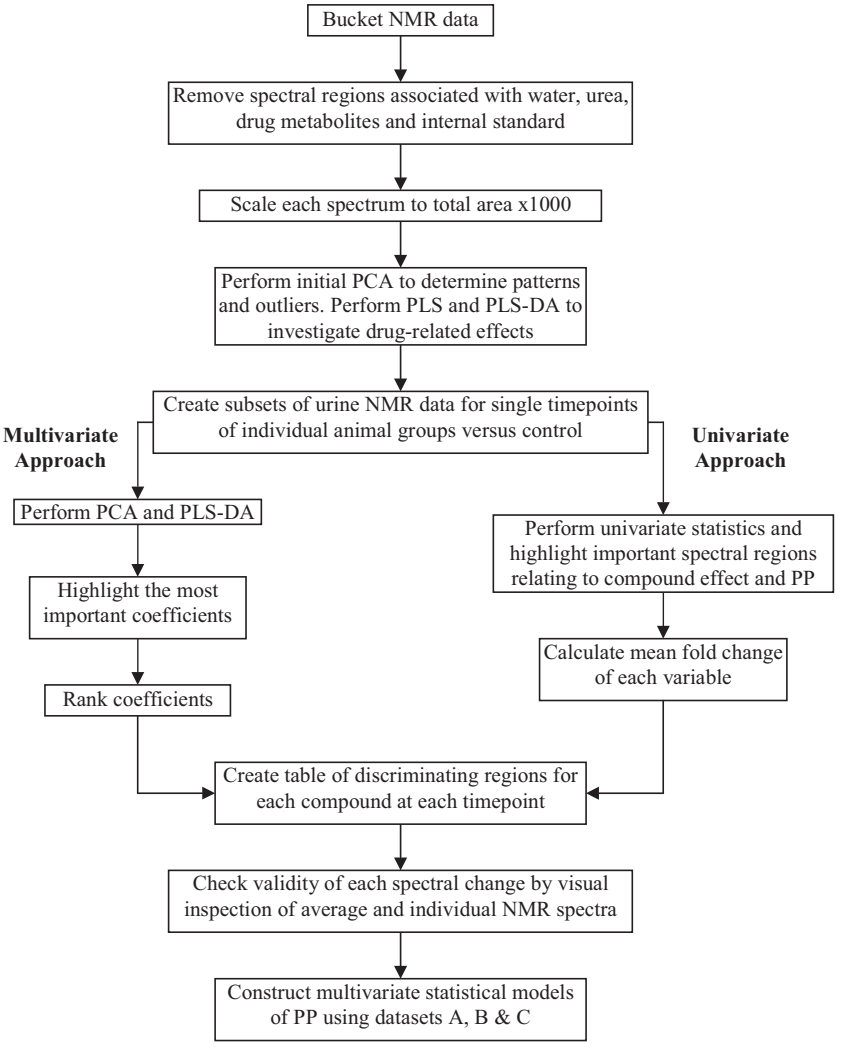

Figure 1. Flow Chart outlining the procedure used to construct multivariate statistical models of PP.

observed and predicted values; a simple way of visualizing this was by fitting a regression line to the observed versus predicted values for the initial model and the predicted values. The difference in slope of the line was an indication of how well the model performed for this dataset.

A totally independent test set from a different study (Test Study) was then used to further validate the model and predict peroxisome counts. For the Test Study, observed peroxisome counts were available for all animals in the control and fenofibrate-treated groups. Only Dataset C was used for this test to reduce the impact on the predictions errors of the spectral regions that contained inherent variability between strains believed to be unassociated with PP.

Results

Body weights, liver weights and clinical chemistry parameters

Adverse clinical signs such as weight loss were not observed for any of the compounds studied, although a statistically significant reduction in body weight

gain (at the 5% level) was observed for GWA, GWB and fenofibrate. GWC caused an increase in body weight gain relative to controls (Ringeissen *et al.* 2003). The major clinical chemistry findings are summarized in table 5.

Measurement of PP using Relative Liver Weight (RLW) and TEM-derived peroxisome counts (Pxc) of liver sections.

The mean number of peroxisomes per cell for each treatment was calculated for the periportal and centrilobular hepatic regions. There was a wide variation between cells of the same treatment group in the number of peroxisomes per cell, both in the same animal and between the two animals examined per group. The following limits were arbitrarily applied in order to exclude the possibility that differences were only due to sampling variation. An increase greater than 100% above the control values was considered to be due to treatment; one between 50 and 99% possibly due to treatment; and less than 50% not due to treatment. Within these constraints, PP was seen in the Main study with GWA, GWB and fenofibrate at high dose (HD) and possibly with fenofibrate at low dose (LD). Low doses of GWA and GWB did not induce PP, nor did a low or high dose of GWC. In the Test study PP was observed for fenofibrate-dosed animals but not controls (table 6).

There were a greater number of peroxisomes in the control cells examined from the centrilobular region compared to those from the periportal region. It is uncertain, within the constraints of the methods used, whether the periportal and centrilobular areas differ in their sensitivity to a given peroxisome proliferator or if the treatment-related increase in centrilobular peroxisomes, expressed as % control, simply reflects the greater number of peroxisomes in this area.

NMR data analysis

NMR and liquid chromatography/mass spectrometry (LC/MS) analysis highlighted several spectral regions that may relate to fenofibrate metabolites in the NMR spectra. These regions were excluded from the dataset for fenofibrate-treated rat samples. No drug metabolites were detected in the urine using LC/MS for compounds GWA, GWB and GWC (Ringeissen *et al.* 2003).

Differences in spectral patterns related to GWA, GWB, GWC and fenofibrate activity (Main Study)

Univariate statistical analyses

Univariate statistical data analysis was carried out to provide supporting evidence for the MVDA. The *t*-test *p* values were obtained at each timepoint (56–168 h) for all variables relative to controls. The spectral regions that were significantly different between treatments were highlighted. In all cases, biomarker selection was based on the MVDA results and spectral regions highlighted by PLS-DA. The selected regions were subsequently validated by spectral comparison and in most cases gave a *t*-test *p* value of $p < 0.05$.

Table 5. Summary of liver and body weights at autopsy, and clinical chemistry parameters for the Main Study that showed significant changes after 7 days repeat dosing (reproduced from Ringeissen *et al*. 2003).

Test Material	Control	GWA		GWB	GWC		Fenofibrate		
Dose[a]	N/A	LD	HD	LD	HD	LD	HD	LD	HD
Body weight gain (g), Day 0–7	19.84	22.38	11.74	22.26	16.4	31.42	35.56	23.12	16.02
Liver weight (g) on Day 7	Control				(% Change from control)				
	10.94	+6	+35**	+2	+39**	−8	−12*	+2	+40**
Clinical Chemistry (Plasma) on Day 7									
ALP (IU/L)	328.0	371.4	528.2**	469.4*	454.2*	350.8	324.0	353.4	440.6
ALT (IU/L)	37.10	42.20	47.00**	40.70	33.70	47.30	42.70	34.60	44.10*
AST (IU/L)	53.90	60.70	70.60**	61.40	54.70	74.60*	72.30*	67.00*	69.90*
Albumin (g/L)	38.50	41.22	45.98**	38.62	42.76*	39.04	36.68	41.66	43.12**
CHL (mmol/L)	1.440	1.146*	0.640**	1.334	0.960**	1.518	1.718*	0.808**	0.616**
TRG (mmol/L)	1.698	1.036**	0.686**	1.310*	0.752**	0.428**	0.766**	1.168**	0.828**
HDL (mmol/L)	1.270	0.990*	0.518**	1.198	0.840**	1.328	1.460	0.682**	0.476**
LDL (mmol/L)	0.126	0.116	0.088	0.096	0.070*	0.144	0.208**	0.092	0.106

*$p < 0.05$, **$p < 0.01$. [(a)]N/A = Not Applicable; LD = Low Dose; HD = High Dose.

Table 6. Peroxisome counts and Relative Liver Weight data.

Study	Group	Dose	Rat #	Mean Pxc[e]	±StDev[f]	Mean RLW[a]
1	1	Control	1	20	8.5	3.63
			2	19	6.1	
	2	GWA LD	6	20.5	7.9	3.84
			7	19	7.1	
	3	GWA HD	13	41[b]	16.9	4.91[(c⋆⋆)]
			14	48.5[b]	14.3	
	4	GWB LD	16	23	8.5	3.68
			17	28	8.4	
	5	GWB HD	22	59.5[b]	18.9	5.00[(c⋆⋆⋆)]
			23	53[b]	22.5	
	6	GWC LD	26	22.5	8.5	3.34
			27	21.5	7.1	
	7	GWC HD	31	25	12.6	3.18[(d⋆)]
			32	19.5	7.4	
	8	FEN LD	36	38	15.0	3.69
			38	30.5	8.6	
	9	FEN HD	41	68.5[b]	19.9	5.08[(c⋆⋆⋆)]
			43	57[b]	20.3	
2	1	Control	1	15.6	5.8	3.85
			5	11.1	3.3	
	2	FEN	7	75.5[b]	27.6	6.06[(c⋆⋆⋆)]
			9	74.6[b]	20.9	

[a]Relative liver weights (RLW) were obtained by dividing liver weight by the body weight for each animal.
[b]PP is suggested when there is >2-fold increase in Pxc relative to control, an arbitrary threshold.
[c]Significant increase in relative liver weight.
[d]Significant decrease in relative liver weight.
[e]Mean Pxc = Average peroxisome number per hepatocyte.
[f]StDev = standard deviation of the mean.
[c]and [d]were measured using a two-tailed Student's *t*-test assuming unequal variance (⋆$p < 0.05$, ⋆⋆$p < 0.001$, ⋆⋆⋆$p < 0.0001$ – significance cut-offs chosen for consistency with NMR analysis).

Multivariate statistical analyses

Preliminary PCA of Main Study Dataset A revealed some clustering of the different dose groups. A small number of samples appeared as outliers due to poor quality spectra arising from NMR acquisition or processing errors. These factors were identified using the contributions and loadings plots from the PCA and by visual inspection of the spectra. Some outlying samples were contaminated by bacterial and/or fungal growth, manifested by an increase in formate or ethanol and occasionally increased levels of acetate, succinate, lactate and methylamines.

During the acclimatization period the urine sample composition appeared more variable both by PCA and by spectral comparison. The variation appeared to be due to a temporary increase in urinary glucose and decreased tricarboxylic acid (TCA) cycle intermediates, creatine, creatinine and taurine in some animals, all of which were reduced in variability after 3 days in metabolism cages. This is consistent with previous findings in-house, confirming the need for at least a 3-day acclimatization period for rats in metabolism cages.

PCA of 56–168 h post-dose Main Study Dataset A, minus degraded samples and poor quality spectra, showed that Group 3 (table 1) samples were partly

separated from controls in PC1 (principal component 1) due to glycosuria and Group 4 samples were separated in PC2 due to a decrease in TCA cycle metabolite excretion (data not shown). Repetition of the PCA of the high dose samples alone for easier visualization showed additional partial groupings. The groupings were based mainly on high variation in TCA cycle and taurine. Whilst these and other spectral regions highlighted in table 7 are clearly influenced by drug treatment, they are non-specific biomarkers of toxicity/disease/dietary intake/body weight change which have been highlighted by most previous studies and give no further insight into any biochemical sequelae of PPAR agonist activity. As these spectral regions showed no correlation with PP or RLW (univariate or multivariate), additional PLS models were constructed using Main Study Dataset B (with tricarboxylic acid cycle intermediates, taurine, hippurate, and chlorogenic acid metabolites deleted; table 7) as well as Dataset A.

PCA of the Main Study Dataset B showed clustering of the dose groups in PCs 2 and 4 (figure 2A). PLS-DA was then carried out on Dataset B in order to define further the differences between the dose groups (figure 2B). The principal component scores plot describing the PLS-DA indicated five distinct clusters of urine samples in PC1 and PC2. These clusters described the NMR data which related to control animals (C; red), GWA (1; light blue), GWB (2; purple), GWC (3; dark blue) and fenofibrate (4; green). As the corresponding loadings plot (data not shown) described both positive and negative correlations it was then necessary to separately analyse each compound relative to control. In the case of each compound a clear separation was observed for samples collected after 56 h post-dose, although GWC samples resembled controls from day 4 onwards. The first component in each model was significant, confirming that the NMR data contained information about the dose group. This accounted for 45, 47, 39 and 47% of the variance in the NMR data for GWA (1), GWB (2), GWC (3) and fenofibrate (4), respectively, (figure 3A–D).

After comparison of the sorted coefficient lists from PLS-DA of each compound relative to control it was found that there were several metabolite regions that were common to GWA, GWB and fenofibrate but not GWC. These included *N*-methylnicotinamide (NMN) and *N*-methyl-4-pyridone-3-carboxamide (4PY), the regions tentatively assigned to metabolite precursors of NMN and 4PY (figure 4), dicarboxylic acids and a low molecular weight globular protein. The spectral regions most associated with GWC activity, including glucose, maltose and unassigned sugars, were not associated with GWA, GWB and fenofibrate samples.

Detailed analysis of average urine NMR spectra

Comparing the univariate and multivariate results showed that the majority of the high ranking coefficients also had a low associated *t*-test *p* value ($p < 0.05$). A detailed analysis was then carried out using average spectra from each dose group at each time point compared to the vehicle-dosed spectra to confirm the validity of the changes observed in the univariate and multivariate statistical analyses. The majority of spectral regions with high ranked coefficients from pareto-scaled

Table 7. Summary of the down-weighted spectral regions for the reduced PP prediction models.

Metabolite	Reasons for deletion
Tricarboxylic acid cycle intermediates	Correlation analysis confirmed that no significant correlation was observed between TCA cycle intermediates and any of the PP measures. Both in-house and published data have shown that TCA cycle intermediates are non-specific effects altering with age, strain, species, sex, diet, food intake, weight loss, various toxins and various genetic modifications (Nicholson and Wilson 1989, Anthony *et al.* 1994, Beckwith-Hall *et al.* 1998, Sweatman *et al.* 2001, Stanley 2003). Larger alterations have been shown to indicate renal tubular acidosis (Gartland *et al.* 1988).
Taurine	PC plots showed high non-group-dependent variation. No correlation was observed with PP measures. Previous studies have shown that taurine levels alter with food intake, diet and weight loss (Sweatman *et al.* 2001). Substantial changes in taurine (much greater than the mean fold changes observed in the present study) have been noted following exposure to various liver toxins (Sanins *et al.* 1990).
Hippurate	PC plots showed high non-group-dependent variation and correlation analysis confirmed no correlation with PP endpoints. Hippurate levels have been shown previously to change with food intake and diet and may be reflecting changes in gut microflora populations (Phipps *et al.* 1998, Gavaghan *et al.* 2001). Alterations in the relative proportions of hippurate and cinnamic acid derivatives have been observed in previous in-house studies for the same animal within the same experiment in a non-group-dependent manner.
Drug-related resonances	As these were not relevant to an endogenous biomarker study, they were deleted from the dataset at outset.
Urea	Urea measurement may reflect changes in sample pH, sample degradation and efficiency of water suppression, and was therefore deleted from the dataset at the outset.
Glycosuric samples	Major outlying samples dominating the first PC were deleted before PLS-DA. Previous in-house studies have shown that glucose excretion increases during the acclimatization period, probably in response to increased stress. Glycosuria has been observed in renal and hepatotoxicity as well as diabetes and in the present study it was characteristic of GWC effects. Initial PLS-DA models incorporated this region of the spectrum with outlying samples deleted to determine its influence on the Y variables. Glucose and unassigned sugar changes were strongly associated with GWC activity but not with PPARα activity or PP so it was therefore decided to delete the glucose region from the reduced dataset models.
meta-hydroxyphenylpropionic acid/cinnamic acid derivatives	These have been shown previously to be non-specific markers that change with food intake and body weight loss (Sweatman *et al.* 2001, Gray *et al.* 2003). Changes in dietary content lead to changes in urinary concentration. The ratio of these metabolites to hippurate probably reflect changes in gut microflora in a non-group-dependent pattern in this study.

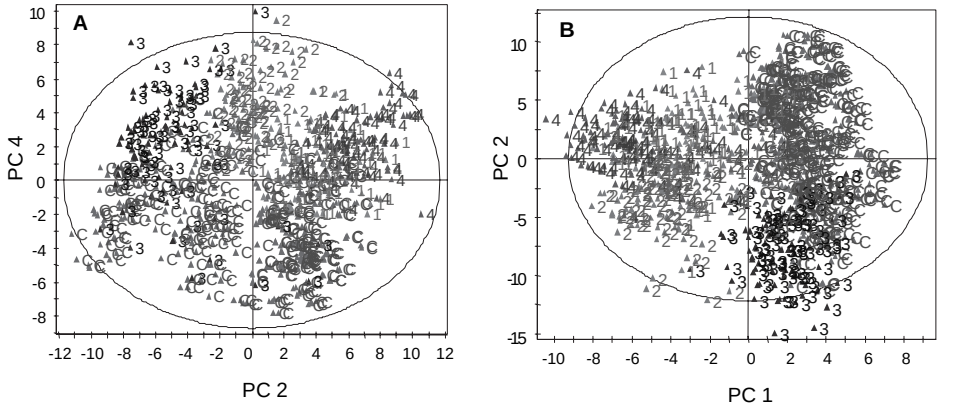

The scores plots for the PCA analysis (A) showed some partial clustering of controls in PC4 and the different PPAR groups in PC2, although groups 1 and 4 (GWA and fenofibrate) did not resolve. In the PLS-DA scores plots, there were distinct clusters for all 4 groups and the controls in the first 2 PC's. For the PCA analysis the cumulative R^2 value for the first 4 components was 61%. For the PLS-DA analysis the R^2X, R^2Y and Q^2 were 28%, 25% and 25% respectively. Key: C = control; 1 = GWA; 2 = GWB; 3 = GWC; 4 = Fenofibrate

Figure 2. Scores plots showing PCA (A) and PLS-DA (B) results of the pareto-scaled Main Study Dataset B (With Hotelling's T^2 ellipse(0.05)).

PLS-DA and with a *t*-test $p < 0.05$ for the unscaled data showed a visible alteration in the NMR spectra (figure 4). The UV-scaled dataset typically contained several areas of baseline as well as peaks of interest.

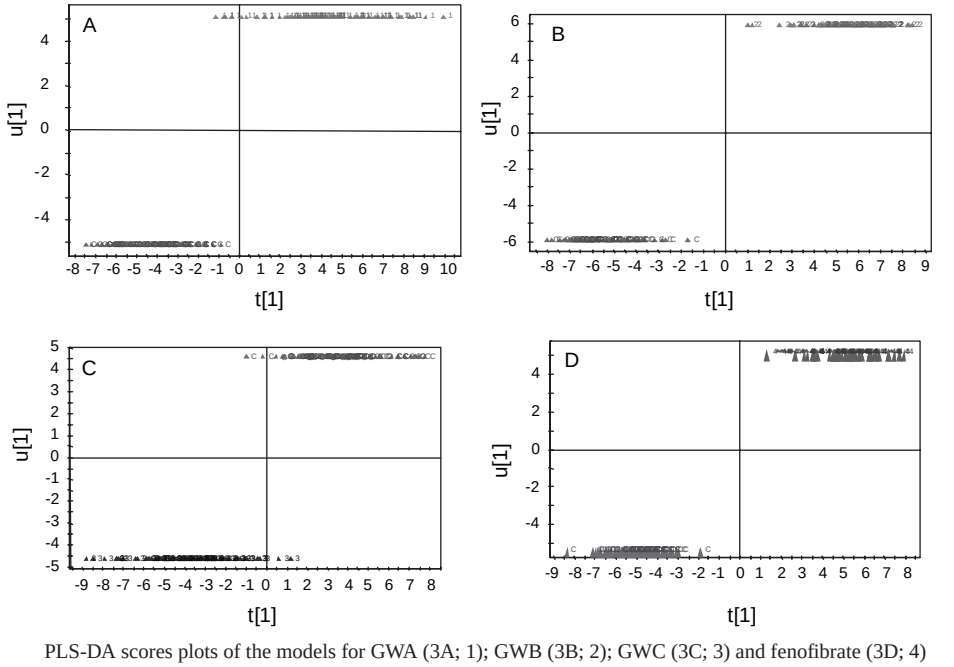

PLS-DA scores plots of the models for GWA (3A; 1); GWB (3B; 2); GWC (3C; 3) and fenofibrate (3D; 4) against controls (3A-D; C).

Figure 3. Principal Component plots showing the scores associated with the PLS-DA analysis of the Main Study Dataset B.

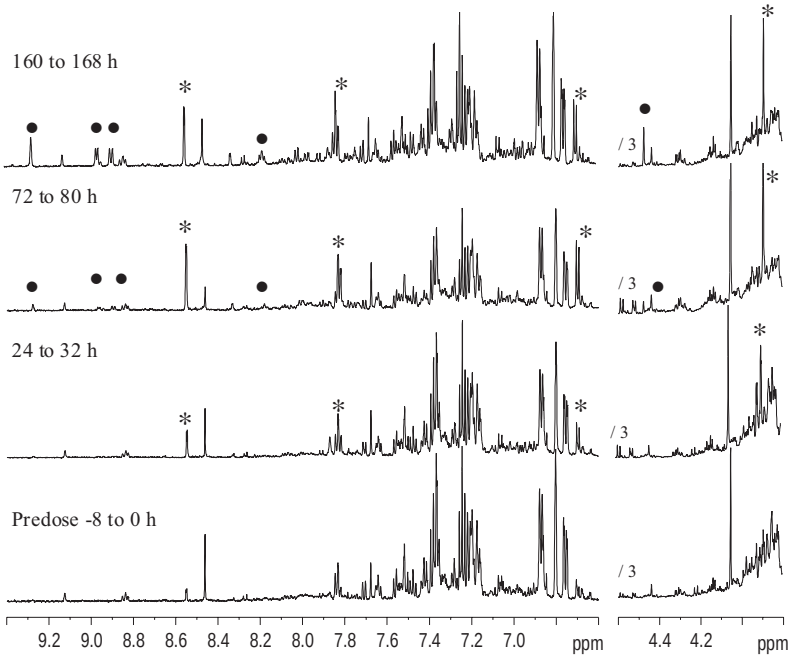

A comparison of the pre- and post-dose urine spectra showed changes in levels of N-methylnicotinamide (•) and N-methyl-4-pyridone-3-carboxamide (*). Changes in aliphatic signals, including a dicarboxylic acid were also observed (data not shown) key: /3: Signal intensity divided by 3.

Figure 4. Main study NMR spectra of urine from a high dose fenofibrate-treated animal pre- and post-dose.

Constructing PLS models of PP

PLS models were constructed for predicting PP from the NMR data using peroxisome count by TEM as the "gold-standard" endpoint and the NMR data from the 152, 160 and 168 h samples. The terminal time-points were chosen for the model construction because peroxisome count is known to increase over time with dosing. Therefore the terminal urine samples would have the strongest correlation with peroxisome count. The first models were constructed using the Main Study Datasets A and B and the results for the 152 h models are summarized in figure 5A and 5B, respectively. An additional set of models was also constructed using Main Study Dataset C, which contained only 42 spectral regions out of the original 280, all of which were influential in the PLS-DA models for PPARα/δ activity (GWA, GWB and fenofibrate) but not PPARγ activity (GWC) (figure 5C). Table 8 details the predictive ability of the different PLS models using RLW and/or Pxc as pathology endpoints.

In order to test the PP model further, predictions of Pxc for a completely independent dataset from a separate (test) study were obtained. This validation was done using the Main Study Dataset C to construct the original model (figure 6, table 9). The spectral regions showing the most influence on the PLS models of PP are highlighted in table 10.

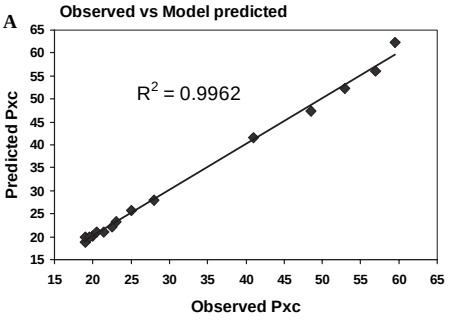

The model had a cumulative R^2X 76%; R^2Y 99.6% and Q^2 96.5% (5 components)

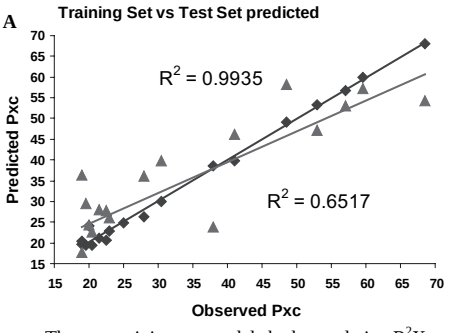

The two training set models had cumulative R^2X 83.4; R^2Y 99.1%; Q^2 89.1% (4 comps) & R^2X 63.8; R^2Y 99.7%; Q^2 84.5% (3 comps).

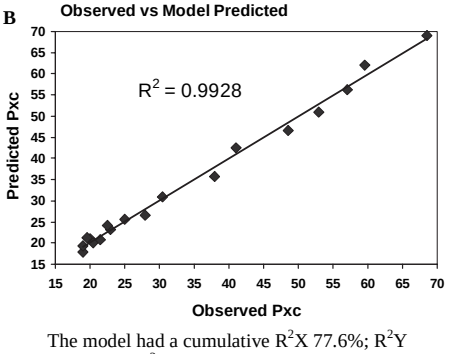

The model had a cumulative R^2X 77.6%; R^2Y 99.3% and Q^2 91.9% (5 components).

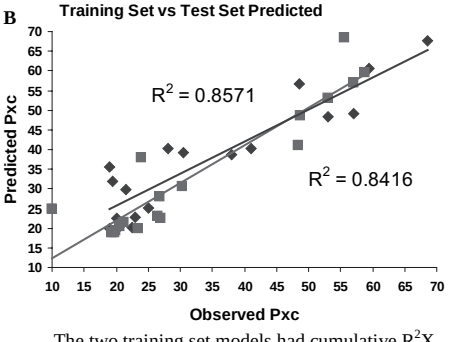

The two training set models had cumulative R^2X 84; R^2Y 99.4%; Q^2 92.4% (4 comps) & R^2X 67; R^2Y 99.9%; Q^2 91.2% (3 comps).

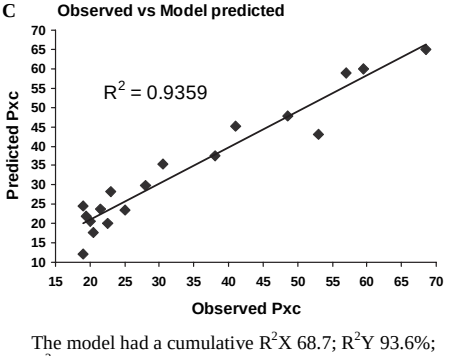

The model had a cumulative R^2X 68.7; R^2Y 93.6%; Q^2 89.1% (3 components).

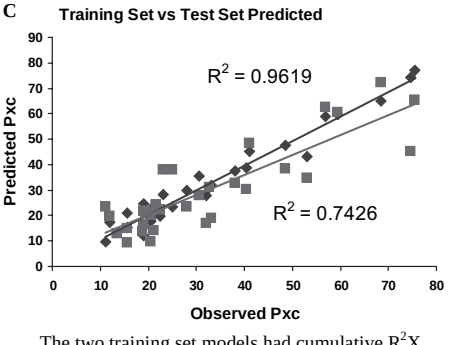

The two training set models had cumulative R^2X 85.3; R^2Y 99%; Q^2 91.2% (2 comps) & R^2X 81, R^2Y 99%, Q^2 86.3% (3 comps).

(1) Two worksets were created using the first and second animal per group respectively. One PLS model was then constructed for each workset (training set) and the other workset used as a test set.

◆ Training set

■ Test set

Figure 5. Predicting Peroxisome count (Pxc) using (A) the full 152 h NMR dataset; (B) the 152 h dataset minus non-specific variables and (C) the 168 h dataset containing only PPARα/δ-associated variables(1).

Table 8. Peroxisome count (Pxc) and peroxisome proliferation (PP) prediction using NMR datasets A, B and C (152 h). Validation for the Predictive models is summarized in figure 5.

		Predictive model used				
Group	Pxc by TEM	A	B	C	RLW	Predicted PP
Control	20.0	20	21	20	3.9	No PP
Control	19.0	19	18	12	3.2	No PP
Control	–	19	21	23	3.7	No PP
Control	–	22	19	10	3.7	No PP
Control	–	16	17	16	3.6	No PP
GWA LD	20.5	21	20	18	3.8	No PP
GWA LD	19.0	20	19	25	4.1	No PP
GWA LD	–	38	38	30	3.8	No PP
GWA LD	–	27	27	28	3.9	No PP
GWA LD	–	28	28	18	3.6	No PP
GWA HD	–	18	24	52	4.5	PP
GWA HD	–	36	36	48	4.9	PP
GWA HD	41.0	42	42	45	4.7	PP
GWA HD	48.5	47	47	48	5.4	PP
GWA HD	–	35	34	38	5.1	PP
GWB LD	23.0	23	23	28	3.9	No PP
GWB LD	28.0	28	27	30	3.8	No PP
GWB LD	–	22	24	28	3.8	No PP
GWB LD	–	30	30	27	3.3	No PP
GWB LD	–	34	33	35	3.6	No PP
GWB HD	–	43	43	40	5.0	PP
GWB HD	59.5	62	62	60	5.1	PP
GWB HD	53.0	52	51	43	5.2	PP
GWB HD	–	43	42	45	4.8	PP
GWB HD	–	43	44	45	4.9	PP
GWC LD	22.5	22	24	20	3.3	No PP
GWC LD	21.5	21	21	24	3.0	No PP
GWC LD	–	26	26	23	3.2	No PP
GWC LD	–	25	24	21	3.7	No PP
GWC LD	–	26	26	28	3.5	No PP
GWC HD	25.0	26	25	23	3.2	No PP
GWC HD	19.5	20	21	22	3.1	No PP
GWC HD	–	21	20	15	3.5	No PP
GWC HD	–	21	20	22	3.1	No PP
GWC HD	–	24	24	22	3.1	No PP
FEN LD	38.0	36	36	37	4.1	No PP
FEN LD	–	25	27	29	3.4	No PP
FEN LD	30.5	30	31	35	3.9	No PP
FEN LD	–	27	26	34	3.1	No PP
FEN LD	–	26	29	38	3.8	No PP
FEN HD	68.5	68	69	65	5.1	PP
FEN HD	–	51	47	50	5.0	PP
FEN HD	57.0	56	56	59	5.1	PP
FEN HD	–	65	66	68	5.4	PP
FEN HD	–	55	52	52	4.9	PP

Discussion

Clinical chemistry and pathology data

Plasma clinical chemistry results indicated significant dose-related reductions in plasma cholesterol, triglycerides, LDL and HDL following treatment with GWA and GWB. These changes were considered to reflect an alteration in lipid metabolism due to the pharmacological activity of the test material. In addition, reductions in body weight gain and a significant increase in plasma

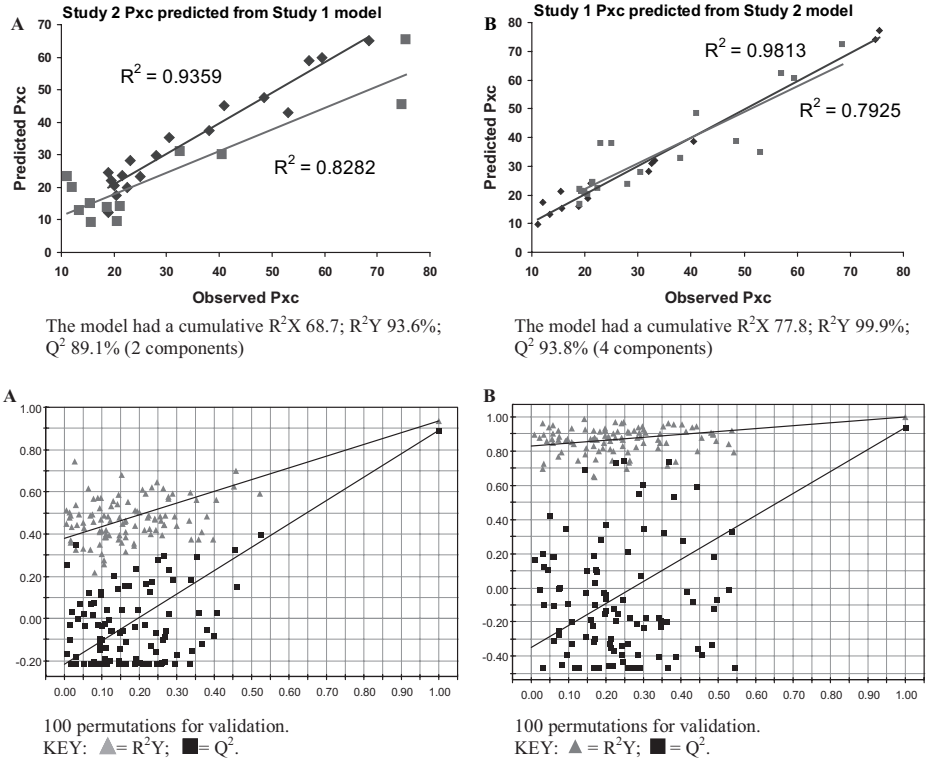

Figure 6. Prediction of Peroxisome count (Pxc) for A) study 2 using study 1 data as the model training set and B) study 1 using study 2 data as the model training set.

albumin concentration were reported with these two compounds. The same changes were observed in animals treated with fenofibrate, except that there was no decrease in plasma LDL in this group. The increases plasma enzyme levels (ALP, ALT and AST) were thought to be consistent with liver hypertrophy and not related to overt hepatocellular damage. The increase in relative liver weights and TEM changes showing a greater than two-fold increase in peroxisome

Table 9. Peroxisome count (Pxc) and peroxisome proliferation (PP) prediction for the Test study using the Main Dataset C model (152 h).

Group	Observed Pxc	Predicted Pxc	RLW	Observed PP	Predicted PP
Control	15.6	9	3.7	no PP	No PP
Control	17.6	7	4.2	no PP	No PP
Control	18.0	14	3.4	no PP	No PP
Control	19.0	25	3.9	no PP	No PP
Control	11.1	23	3.9	no PP	No PP
FEN	72.0	52	5.8	PP	PP
FEN	75.5	65	6.1	PP	PP
FEN	64.6	40	5.8	PP	PP
FEN	74.6	45	6.3	PP	PP
FEN	72.0	50	6.3	PP	PP

Table 10. Spectral regions with high PLS coefficients showing correlation with peroxisome counts.

NMR Chemical Shift Region	Assignment	Correlation Coefficient	Correlation Coeff. t-test p values
9.46	unassigned protein	0.67	0.0485
9.26	*N*-methylnicotinamide (NMN)	0.96	0.0000
9.22	unassigned protein	0.91	0.0007
9.06	unassigned protein	0.55	0.1210
9.02	unassigned protein	0.47	0.1980
8.98	NMN, plus related metabolites	0.95	0.0001
8.94	NMN, plus related metabolites	0.95	0.0001
8.90	NMN	0.97	0.0000
8.86	*N*-methylnicotinic acid	0.90	0.0010
8.82	*N*-methylnicotinic acid	0.44	0.2415
8.78	unassigned protein	0.88	0.0017
8.74	nicotinamide-*N*-oxide	0.89	0.0011
8.70	nicotinurate/nicotinamide	0.89	0.0014
8.54	4PY	0.48	0.1880
8.50	nicotinamide-*N*-oxide	0.64	0.0636
8.34	2PY	0.84	0.0041
8.26	nicotinurate/nicotinamide	0.36	0.3423
8.18	NMN	0.96	0.0000
7.78	several (4PY, nicotinamide-*N*-oxide)	0.81	0.0084
7.74	several (4PY, nicotinamide-*N*-oxide)	0.91	0.0007
6.66	*N*-methyl-2-pyridone-5-carboxamide	0.44	0.2301
5.38	allantoin	−0.66	0.0519
4.50	NMN	0.64	0.0636
4.46	NMN, *N*-methylnicotinic acid	0.90	0.0010
2.18	dicarboxylic acid (>C7)	−0.75	0.0190
1.58	dicarboxylic acid (>C7)	−0.75	0.0200
1.54	dicarboxylic acid (>C7)	−0.76	0.0165
1.30	dicarboxylic acid (>C7)	−0.76	0.0184
0.78	unassigned protein	0.61	0.0792
0.74	unassigned protein	0.64	0.0657
0.70	unassigned protein	0.67	0.0461
0.58	unassigned protein	0.92	0.0005
0.54	unassigned protein	0.93	0.0002
0.46	unassigned protein	0.91	0.0008
0.42	unassigned protein	0.95	0.0001
0.22	unassigned protein	0.89	0.0015
−1.3	singlet from unassigned protein	0.61	0.0807

t-test $p < 0.05$ are highlighted. Assignments were obtained from Fan *et al.* (1996) and Lindon *et al.* (1999). The unassigned protein had a similar NMR profile to α-2-microglobulin, identified in male mouse urine by one-dimensional gel and tryptic-digest LC/MS/MS (in-house data not shown).

count observed with GWA, GWB and fenofibrate were considered to be consistent with PP.

NMR data

Previous work on the Main study has highlighted the possibility of NMN and 4PY as putative markers of PP (Ringeissen *et al.* 2003). Both of these metabolites have been the subject of further investigation in an attempt to validate their use as markers of PP. The MVDA in the current study showed that there were also several other regions of the NMR spectrum as well as NMN and 4PY which correlated to PPARα and PPARδ agonist activity (but not PPARγ agonist activity). PPARγ

agonist activity was described by a different set of variables, mostly contained within the sugar/carbohydrate region of the spectrum. The purpose of this present investigation was to determine the time course of the PPARα- and PPARδ-related spectral changes in relation to PP and hence which of these regions may be part of a pattern of potential markers of PP and other PPAR-related activities and/or toxicity.

The outcome of the current more detailed data evaluation has resulted in the discovery of up to 97 regions of the spectrum that were altered in response to PPAR agonist administration (PPARα, PPARδ and PPARγ). Forty-two of these regions appeared to be altered after administration of the PPARα and PPARδ agonists and fenofibrate but were either absent or negligibly altered for the PPARγ agonist. The remainder were mostly spectral regions relating to sugars. The PPARγ agonist was the negative control in this study (*i.e.* a PPAR agonist compound with no observed PP) and the inference from the comparison of the different PPAR agonists is that these 42 regions may be potential biomarkers of PP. These metabolites may be biomarkers in their own right, or could be used as a pattern of changes that can be incorporated into predictive models of PP. Subsequent MVDA regression techniques were performed and these confirmed that between 36 and 42 of these regions showed a high linear correlation to PP, producing a statistical model which could potentially predict PP to more than 98% accuracy.

Assessment of Pxc by TEM highlighted a wide variation in counts between cells of the same treatment group. This was the case both within the same animal and between the two animals. As a result it was necessary to apply generous limits when determining whether the increases were related to treatment. This was to exclude the possibility that differences were only due to sampling variation.

Model validation, by dividing the Main study data into training and test sets, showed that both of the reduced dataset models more accurately predicted PP (in terms of a two-fold increase in Pxc) than the full NMR dataset. Over-fitting of the data becomes increasingly likely when variables are selected based on their statistics within the same study, although it is less of a problem if selection is carried out using prior biochemical knowledge of the variables from previous studies. As both methods of selection were used in this study for the reduced models, it was important to test for model over-fit. This was done using a completely independent Sprague Dawley Test study. This was a particularly stringent test for over-fit as it incorporated an evaluation of the model performance over 2 different rat strains as well as two separate studies. Using the Wistar Han dataset to construct training models it was possible to accurately predict the presence or absence of PP (above or below a two-fold control threshold) in all Sprague Dawley rats. This validation was done primarily for the 42 bucket model, which used only 15% of the original data, because this was potentially the model where most over-fit could occur. There are also inherent differences in the urine profile of Wistar Han and Sprague Dawley rats and the reduced model had the advantage over the complete models (containing more NMR variables) of not including these regions of high variation. The difference in field strength (600 MHz versus 700 MHz for the Main and Test

studies, respectively) had little impact on the prediction of the test set, possibly because the majority of the "discriminating" regions altered substantially in peroxisome-proliferated rats compared to controls.

The spectral regions contributing most to the statistical model have been tentatively identified with reference to literature and in-house information. It appears that some of the regions may correspond to other metabolites in the tryptophan-NAD^+ pathway, many of which are not normally detected by ^{1}H-NMR in control urine. Their presence in the urine of rats undergoing PP and their direct correlation with the peroxisome counts adds further weight to the hypothesis that the up-regulation of QAPRT ($\sim$2 fold) and more importantly the down-regulation of ACMSD ($\sim$11 fold) are reflecting PP in the rat (Ringeissen *et al.* 2003).

Other influential regions of the spectrum (in terms of PP) include those related to dicarboxylic acids, which show a strong negative correlation with PP. This may be as a result of the down-regulation of ACMSD, which directly affects the glutarate pathway and thus the metabolism of various dicarboxylic acids. The assignments of these dicarboxylic acid metabolites are yet to be elucidated. A globular protein component, tentatively assigned to an alpha-2 microglobulin, also appears from day 3 onwards in the study, possibly increasing in concentration and directly correlating with the peroxisome counts.

The spectral regions identified in this investigation may be used to create more widely applicable predictive models once differences in metabolite flux in individual pathways between species have been addressed. To do this it would be necessary to evaluate the individual components of the model for Sprague Dawley rats and extend the studies to other species such as human and non-human primates, with the caveat that less background information is available for the pathways in question in primates.

References

Anthony, M. L., Sweatman, B. C., Beddell, C. R., Lindon, J. C. and Nicholson, J. K. 1994, Pattern recognition classification of the site of nephrotoxicity based on metabolic data derived from proton nuclear magnetic resonance spectra of urine. *Molecular Pharmacology*, **46**, 199–211.

Ashby, J., Brady, A., Elcombe, C. R., Elliott, B. M., Ishmael, J., Odum, J., Tugwood, J. D., Kettle, S. and Purchase, I. F. H. 1994, Mechanistically-based human hazard assessment of peroxisome proliferator-induced hepatocarcinogenesis. *Human & Experimental Toxicology*, **13** (Supplement 2), S1–S117.

Beckwith-Hall, B. M., Nicholson, J. K., Nicholls, A. W., Foxall, P. J. D., Lindon, J. C., Connor, S. C., Abdi, M., Connelly, J. and Holmes, E. 1998, Nuclear magnetic resonance spectroscopic and principal components analysis investigations into biochemical effects of three model hepatotoxins. *Chemical Research in Toxicology*, **11**, 260–72.

Bentley, P., Calder, I., Elcombe, C., Grasso, P., Stringer, D. and Wiegand, H. J. 1993, Hepatic peroxisome proliferation in rodents and its significance for humans. *Food Chemical Toxicology*, **31**, 857–907.

Brown, P. J., Winegar, D. A., Plunket, K. D., Moore, L. B., Lewis, M. C., Wilson, J. G., Sundseth, S. S., Koble, C. S., Wu, A., Chapman, J. M., Lehmann, J. M., Kliewer, S. A. and Willson, T. M. 1999, A Ureido-Thioisobutyric Acid (GW9578) is a subtype-selective PPARα Agonist with Potent Lipid-Lowering Activity. *Journal of Medicinal Chemistry*, **42**, 3785–3788.

Bybee, A., Styles, J. A., Beck, S. L. and Blackburn, D. 1990, Mitosis and histopathology in rat liver during methylclofenapate induced hyperplasia. *Cancer Letters*, **52**, 95–100.

Fan, T. W.-M. 1996, Metabolite profiling by one- and two-dimensional NMR analysis of complex mixtures. *Progress in Nuclear Magnetic Resonance Spectroscopy*, **28**, 161–219.

GARTLAND, K. P. G., BONNER, F. W. and NICHOLSON, J. K. 1988, Investigations into the biochemical effects of region-specific nephrotoxins. *Molecular Pharmacology*, **35**, 242–250.

GAVAGHAN, C. L., NICHOLSON, J. K., CONNOR, S. C., WILSON, I. D., WRIGHT, B. and HOLMES, E. 2001, Directly coupled high-performance liquid chromatography and nuclear magnetic resonance spectroscopic with chemometric studies on metabolic variation in Sprague Dawley rats. *Analytical Biochemistry*, **291**, 245–252.

GRAY, R. A., CONNOR, S. C., HODSON, M. P., CLAYTON, N. M., HASELDEN, J. N. and CHESSELL, I. P. 2003, An NMR-based metabolic profiling study of inflammatory pain using the rat FCA Model, *Pain*, submitted.

LAKE, B. G. 1995a, Mechanisms of hepatocarcinogenicity of peroxisome-proliferating drugs and chemicals. *Annual Review of Pharmacology and Toxicology*, **35**, 483–507.

LAKE, B. G. 1995b, Peroxisome proliferation: urrent mechanisms relating to non-genotoxic carcinogenesis. *Toxicology Letters*, **82/83**, 673–681.

LINDON, J. C., NICHOLSON, J. K. and EVERETT, J. R. 1999, NMR Spectroscopy of biofluids. *Annual Reports on NMR Spectroscopy*, **38**, 1–88.

NICHOLSON, J. K. and WILSON, I. D. 1989, High resolution proton magnetic resonance spectroscopy of biological fluids. *Progress in Nuclear Magnetic Resonance Spectroscopy*, **21**, 449–501.

NICHOLSON, J. K., LINDON, J. C. and HOLMES, E. 1999, Metabonomics: understanding the metabolic responses of living systems to pathophysiological stimuli via multivariate statistical analysis of biological NMR spectroscopic data. *Xenobiotica*, **29**, 1181–1189.

NICHOLSON, J. K., CONNELLY, J., LINDON, J. C. and HOLMES, E. 2002, Metabonomics: a platform for studying drug toxicity and gene function. *Nature Reviews Drug Discovery*, **1**, 153–161.

PHIPPS, A. N., STEWART, J., WRIGHT, B. and WILSON, I. D. 1998, Effect of diet on the urinary excretion of hippuric acid and other dietary-derived aromatics in rat. A complex interaction between diet, gut microflora and substrate specificity. *Xenobiotica*, **28** (5), 527–537.

QUALLS, JR., C. W., HOIVIK, D. J., SANTOSTEFANO, M. J., BROWN, H. R., ANDERSON, S. P., OTT, R. J., MIRABILE, R. C., OLIVER, B. R., MUDD, P. N. and MILLER, R. T. 2003, Fibrates induce peroxisomal and mitochondrial proliferation in cynomolgous monkeys without causing cell cycle alterations or oxidative stress. Annual Meeting, Society of Toxicology. *Toxicological Sciences.*

RINGEISSEN, S., CONNOR, S. C., BROWN, H. R., SWEATMAN, B. C., HODSON, M. P., KENNY, S. P., HAWORTH, R., MCGILL, P., PRICE, M. A., AYLOTT, M. C., M. R., NUNEZ, D. J., HASELDEN, J. N. and WATERFIELD, C. J. 2003, *N*-methylnicotinamide and *N*-methyl-4-pyridone-3-carboxamide: potential urinary and plasma biomarkers of peroxisome proliferation in the rat-identification by ^{1}H NMR and HPLC. *Biomarkers*, **8**(3–4), 240–271.

ROBERTSON, D. G., REILY, M. D., SIGLER, R. E., WELLS, D. F., PATERSON, D. A. and BRADEN, T. K. 2000, Metabonomics: evaluation of nuclear magnetic resonance (NMR) and pattern recognition technology for rapid *in vivo* screening of liver and kidney toxicants. *Toxicological Sciences*, **57**, 326–37.

ROMACH, E. H., SHENK, J. L., OTT, R. J., WILLSON, T. M. and MILLER, R. T. 2002, Hepatic effects of PPARδ are distinct from PPARα. *The Toxicologist*, **66**, 261.

SANINS, S. M., NICHOLSON, J. K., ELCOMBE, C. and TIMBRELL, J. A. 1990, Hepatotoxin-induced hypertaurinuria: a proton NMR study. *Archives of Toxicology*, **64** (5), 407–411.

SLIM, R. M., ROBERTSON, D. G., ALBASSAM, M., REILY, M. D., ROBOSKY, L. and DETHLOFF, L. A. 2002, Effect of dexamethasone on the metabonomics profile associated with phosphodiesterase inhibitor-induced vascular lesions in rats. *Toxicology and Applied Pharmacology*, **193**, 109–16.

STANLEY, E. G. PhD Thesis, 2003, University of London.

SWEATMAN, B. C., MANINI, J. A. and WATERFIELD, C. J. 2001, ^{1}H-NMR analysis of urine in toxicity studies: side effects of reduced feeding. *Toxicology*, **164**, 225.

TUCKER, M. J. and ORTON, T. C. 1995, *Comparative Toxicology of Hypolipidaemic Fibrates* (London: Taylor and Francis).